

Using multifocal plane microscopy to reveal novel trafficking processes in the recycling pathway

Zhuo Gan^{1,2}, Sripad Ram^{1,3}, Raimund J. Ober^{1,3,*} and E. Sally Ward^{1,*}

¹Department of Immunology, University of Texas Southwestern Medical Center at Dallas, Dallas, TX 75390, USA

²Biomedical Engineering Graduate Program, University of Texas Southwestern Medical Center at Dallas, Dallas, TX 75390, USA

³Department of Electrical Engineering, University of Texas at Dallas, Dallas, TX 75080, USA

*Authors for correspondence (sally.ward@utsouthwestern.edu; ober@utdallas.edu).

Accepted 10 December 2012

Journal of Cell Science 126, 1176–1188

© 2013. Published by The Company of Biologists Ltd

doi: 10.1242/jcs.116327

Summary

A major outstanding issue in cell biology is the lack of understanding of the contribution of tubulovesicular transport carriers (TCs) to intracellular trafficking pathways within 3D cellular environments. This is primarily due to the challenges associated with the use of microscopy techniques to track these highly motile, small compartments. In the present study we have used multifocal plane microscopy with localized photoactivation to overcome these limitations. Using this approach, we have characterized individual components constituting the recycling pathway of the receptor FcRn. Specifically, several different pathways followed by TCs that intersect with larger, relatively static sorting endosomes have been defined. These pathways include a novel ‘looping’ process in which TCs leave and return to the same sorting endosome. Significantly, TCs with different itineraries can be identified by associations with distinct complements of Rab GTPases, APPL1 and SNX4. These studies provide a framework for further analyses of the recycling pathway.

Key words: FcRn, Localized photoactivation, Multifocal plane microscopy, Receptor recycling, Transport carrier

Introduction

Intracellular trafficking pathways deliver proteins to the appropriate destination within cells and are therefore critical for cell function and survival. One such pathway is represented by the endolysosomal system involving the internalization of membrane receptors and delivery to sorting endosomes. Following entry into sorting endosomes, transmembrane proteins can be recycled back to the cell surface or enter late endosomal/lysosomal compartments for degradation. Relatively small, highly motile tubulovesicular transport carriers (TCs) of high abundance play an important role in these transport processes (Stenmark, 2009; Lippincott-Schwartz and Phair, 2010). However, despite extensive analyses of intracellular trafficking pathways (Maxfield and McGraw, 2004; Grant and Donaldson, 2009), knowledge of the spatial and temporal behavior of TCs is very limited.

The highly complex network of interconnected pathways that is formed by TCs confounds their analysis. In addition, the longstanding viewpoint that incoming endocytic vesicles fuse with larger early or sorting endosomes following entry into the cell (Griffiths and Gruenberg, 1991; Zerial and McBride, 2001) has more recently been challenged by data indicating that endocytic vesicles can mature into early endosomes by homotypic fusion combined with sequential removal and addition of proteins such as Rab GTPases (Rink et al., 2005; Zoncu et al., 2009). To resolve these issues there is a need for the characterization of TCs and their itineraries at high temporal and spatial resolution. In turn, such studies have relevance to the modulation of specific intracellular pathways for the treatment of human disease.

Although multiple challenges remain, fluorescence microscopy has evolved to become the method of choice for

analyzing intracellular trafficking pathways. For example, the high density of intracellular compartments within a cell results in problems for the unequivocal tracking of objects due to loss of their identity, and this is exacerbated for highly motile TCs. Further, these TCs are relatively small and consequently the fluorescent signal of associated proteins is low, resulting in decay of the signal to undetectable levels within a relatively short time frame. These factors have to date precluded the tracking of the different pathways that individual TCs take in a cellular environment. Difficulty in tracking TC-associated proteins is enhanced when the protein is also present in the cytosol, giving rise to fluorescent haze. In addition, most imaging modalities result in data collection from a single focal plane whereas cells are three-dimensional objects.

Towards addressing the problems associated with the analysis of TC behavior, we have developed multifocal plane microscopy (MUM) (Prabhat et al., 2004; Prabhat et al., 2007; Ram et al., 2008). MUM enables the simultaneous collection of fluorescence signal from different focal planes within a cell and is therefore well suited for the tracking of fluorescently labeled molecules within the three-dimensional cellular environment. Importantly, the use of MUM combined with high frame rates allows highly motile objects such as TCs to be tracked as they migrate between different focal planes. Many of these processes would not be trackable with more conventional imaging modalities such as z-step acquisition. Further, in the current study we have combined MUM with the use of localized photoactivation (Patterson and Lippincott-Schwartz, 2002; Lippincott-Schwartz et al., 2003; Schuster et al., 2011) in a novel dual objective set up called LP-MUM to overcome problems related to loss of identity. This set up allows the selective activation of photoactivatable-GFP

(PAGFP)-labeled proteins (Patterson and Lippincott-Schwartz, 2002) on individual endosomes. The use of this microscopy configuration has enabled the unambiguous tracking of TCs over relatively long time periods in three dimensions within cells.

The recycling Fc receptor, FcRn, is the focus of the current study. FcRn transports IgG within and across cells, resulting in salvage of this cargo from lysosomal degradation (Ober et al., 2004b; Roopenian and Akilesh, 2007; Ward and Ober, 2009). IgG binds to FcRn at the slightly acidic pH of early endosomes, but with very low affinity at neutral pH (Raghavan et al., 1995; Popov et al., 1996). In general, IgG is internalized into cells through fluid phase pinocytosis and delivered to sorting endosomes in which the pH is permissive for FcRn binding. Following binding, the FcRn–IgG complex is recycled back to the cell surface and IgG is released from FcRn during exocytic processes (Ober et al., 2004a; Ober et al., 2004b; Prabhat et al., 2007). IgG can also be delivered by FcRn-mediated transcytosis across polarized cells such as endothelial and epithelial cells (Dickinson et al., 1999; Antohe et al., 2001; Yoshida et al., 2004; He et al., 2008). Consequently, FcRn serves as a global regulator of IgG levels and transport throughout the body (Roopenian and Akilesh, 2007; Ward and Ober, 2009). FcRn is distributed in relatively static 1–2.5 μm sorting endosomes and smaller, highly motile TCs (Ober et al., 2004b). As such, FcRn provides a clear marker for these endosomal compartments in live cells. However, the interaction between these endosomes and smaller TCs in temporal and spatial terms on the recycling pathway is poorly understood for this or any other receptor.

The characterization of TCs on the endosomal recycling pathway by necessity includes an analysis of Rab GTPase associations. Rab GTPases are major players in the regulation of vesicular trafficking within cells (van der Sluijs et al., 1992; Ullrich et al., 1996; Bielli et al., 2001; Zerial and McBride, 2001; Imamura et al., 2003; Pfeffer and Aivazian, 2004; Schonteich et al., 2008; Stenmark, 2009; Horgan et al., 2010). These GTPases act as tethering molecules and recruit effectors that regulate membrane trafficking processes (Sönnichsen et al., 2000; Stenmark, 2009; Hutagalung and Novick, 2011). Rab4 and Rab11 are associated with endosomal recycling processes (van der Sluijs et al., 1992; Ullrich et al., 1996; Sönnichsen et al., 2000; McCaffrey et al., 2001; Pagano et al., 2004; Ward et al., 2005) and are therefore of relevance to the current study. In addition to Rab GTPases, sorting nexins (SNXs) control intracellular sorting by sensing membrane curvature through Bin-Amphiphysin-Rvs (BAR) domains and associating with specific intracellular compartments (Cullen, 2008). SNX4 is of particular relevance to recycling pathways since it has been shown to regulate the transport of the transferrin receptor from sorting to recycling endosomes (Traer et al., 2007).

The adaptor protein containing PH domain, PTB domain and Leucine zipper motif (APPL) proteins are Rab5 effectors associated with early endosomes or macropinosomes (Miaczynska et al., 2004; Zoncu et al., 2009). These compartments transport signaling receptors such as the epidermal growth factor receptor (EGFR) into the cell prior to conversion to EEA1 positive endosomes (Miaczynska et al., 2004; Zoncu et al., 2009). Whether APPL1 can be used to demarcate TCs containing receptors that do not have a signaling function such as FcRn is unexplored. One aspect of our analyses is therefore to investigate whether, and at what stage of intracellular trafficking, APPL1 is associated with FcRn+ TCs.

In the present study we have used a combination of two plane MUM and localized photoactivation to characterize the pathways taken by FcRn+ TCs in 3D. These studies have for the first time, to our knowledge, resulted in the unambiguous identification of distinct intracellular trafficking processes involving highly motile TCs representing components of the recycling pathway. How these TCs intersect with sorting endosomes within the complex and dynamic network of tubulovesicular compartments has also been defined. The different components of the recycling pathway can be identified by analyzing the distribution of APPL1, SNX4, Rab4 and Rab11 on TCs. Significantly, newly formed, cargo-carrying APPL1+ TCs fuse heterotypically with relatively static sorting endosomes following their entry into cells. Further, we have observed a novel ‘looping’ pathway in which TCs move bidirectionally to leave and return to the same endosome. Collectively, these analyses provide a platform for the further interrogation of the recycling pathway.

Results

Multifocal plane imaging enables the tracking of TCs

FcRn is a recycling receptor present on the limiting membrane of EEA1+ early/sorting endosomes of 1–2.5 μm in diameter, providing an identifier for these compartments (Ober et al., 2004b; Gan et al., 2009) (Fig. 1A; supplementary material Movie 1). Our previous studies have shown that Rab5+/EEA1+ sorting endosomes are 1–2.5 μm in size in untransfected HMEC-1 cells, demonstrating that these endosomes are not enlarged due to transfection (Gan et al., 2009). Following endocytic uptake into cells, FcRn+ TCs fuse with these sorting endosomes (Ram et al., 2008). FcRn is subsequently sorted from the endosomes in tubulovesicular TCs that bud off from the limiting membrane (Ward et al., 2005). In supplementary material Movie 1, the movement of large numbers of highly motile, small TCs that sometimes fuse with these sorting endosomes can be seen. The TCs frequently move in and out of the focal plane and, combined with their high density, this precludes unambiguous identification using single plane imaging. The use of MUM (Prabhat et al., 2004; Prabhat et al., 2007) can overcome these problems (Fig. 1B,C). In Fig. 1B, a TC moves between the two focal planes and can be tracked for >1 minute. In Fig. 1C, a TC leaves a sorting endosome and moves from the upper to the lower focal plane (2.7–3.0 s). The current study is directed towards using MUM and in some cases, localized photoactivation, to characterize TCs on the endocytic recycling pathway.

The different itineraries taken by TCs on the recycling pathway can involve a pre-endosomal or post-endosomal sorting step, an interendosomal transfer process and a novel looping pathway

The recycling pathway involving FcRn+ TCs can be broadly defined by four distinct intracellular trafficking processes in HMEC-1 cells that form the focus of analysis in the present study. Early in the process, a pre-endosomal sorting step is observed in which TCs move from the periphery of the cell and fuse with sorting endosomes (Ram et al., 2008). Subsequent trafficking steps can be categorized as follows: a post-endosomal sorting pathway involves migration of the TC to exocytic sites at the plasma membrane (Prabhat et al., 2007). In addition, there are two other pathways in which TCs either migrate between sorting endosomes in interendosomal transfer events (Ober et al., 2004b) or segregate from a sorting endosome and then return to the same

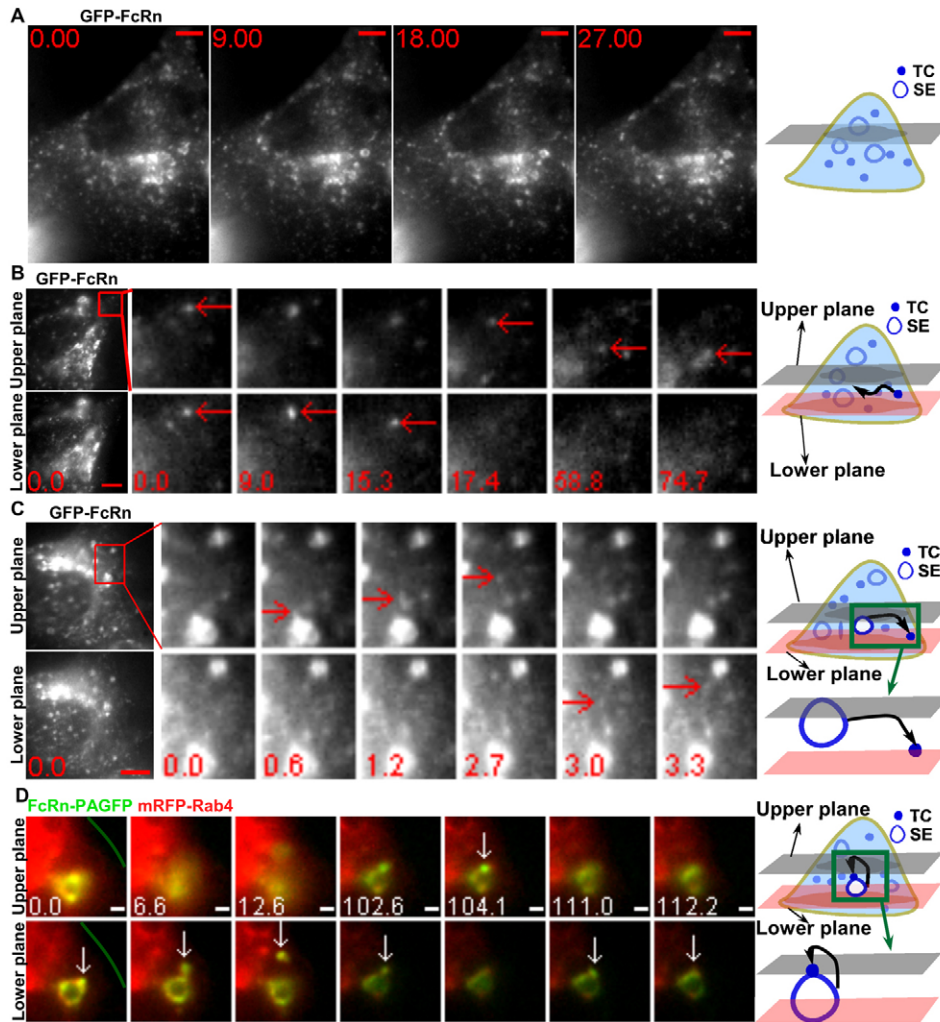


Fig. 1. Multifocal plane imaging enables the tracking of TCs and observation of a novel looping pathway. HMEC-1 cells were cotransfected with GFP-FcRn/ β_2m (A–C) or FcRn-PAGFP/ β_2m /mRFP-Rab4 (D).

Individual images are presented with the time (in seconds) at which each image was acquired (first image is arbitrarily set to time 0). For B and C, the far-left-hand panels show the MUM data for a complete cell, with the boxed regions expanded as cropped images for individual frames. Scale bars: 5 μm (A–C) or 1 μm (D). The green line in D demarcates the plasma membrane. Schematic representations are shown in the right-hand column. Images show selected frames from a dataset continuously acquired at a frame rate of 3 frames per second. (A) Selected frames from supplementary material Movie 1. FcRn can be seen in 1–2.5 μm sorting endosomes (SE) and tubulovesicular TCs. (B) A FcRn+ TC (red arrows) moves between the two focal planes. Two arrows at 0 s indicate a TC seen in both focal planes. (C) A FcRn+ TC (red arrows) leaves a sorting endosome in the upper plane at 1.2 s and moves to the lower plane at 3 s. (D) Selected frames from supplementary material Movie 2. A 405 nm laser beam was focused onto a Rab4+ sorting endosome for ~ 1 s to photoactivate PAGFP. A FcRn+Rab4+ TC (white arrows) extends from a sorting endosome (0–6.6 s) in the lower plane, segregates from this endosome and moves to the upper plane at 104.1 s. Subsequently this TC returns to and merges with the same endosome (111.0–112.2 s).

endosome (Fig. 1D; supplementary material Movie 2). The latter leave and return, or ‘looping’, events have not been described previously.

Looping events involving TCs moving bidirectionally to and from the same sorting endosome usually occur over a relatively long time scale. As a result, to avoid loss of TC identity during imaging the use of localized photoactivation combined with MUM (LP-MUM) is necessary. Fig. 1D shows an example of such a looping event in HMEC-1 cells transfected with FcRn-PAGFP. FcRn-PAGFP on a sorting endosome (labeled with mRFP-Rab4) was photoactivated using a focused 405 nm laser beam with 1 second exposure. An FcRn+ TC leaves this sorting endosome, moves from the lower to upper focal plane (102.6–104.1 s) and returns to the lower plane and fuses with the same sorting endosome. Additional examples of these types of events, and the proteins associated with them, are described below.

TCs on the pre-endosomal sorting pathway have associated APPL1

We initially analyzed pre-endosomal sorting pathways of FcRn+ TCs that precede fusion with sorting endosomes. The involvement of APPL1 in the early endocytic pathway of other receptors such as EGFR (Miaczynska et al., 2004) prompted us to investigate whether APPL1 is also present on FcRn+ TCs that

fuse with these endosomes. HMEC-1 cells were co-transfected with GFP-APPL1 and mRFP-FcRn and imaged as live cells. FcRn+APPL1+ TCs that merge with sorting endosomes were observed (a total of 14 merging TCs were analyzed in different cells from multiple experiments). Fig. 2A (supplementary material Movie 3) shows an example of such a TC that moves from the periphery of the cell and fuses with a sorting endosome.

To investigate whether APPL1+FcRn+ TCs are on a pathway preceding endosomal fusion and sorting rather than a later step of the recycling pathway, cells were pretreated for a relatively short time period with endocytic cargo prior to imaging. HMEC-1 cells were co-transfected with GFP-APPL1 and a mutated variant of FcRn (‘FcRn-mut’ with no fluorescent protein appended, i.e. FcRn-stop) (Prabhat et al., 2007) to allow endocytosis, labeled ligand (IgG) to be tracked. The engineered IgG1, MST-HN (Vaccaro et al., 2005), interacts with FcRn-mut with high affinity ($K_d \sim 10$ nM) at near neutral pH, resulting in receptor-mediated uptake of ligand into cells. Transfected cells were pulsed with Alexa 555-labeled MST-HN to label the pre-endosomal pathway. Of a total of six MST-HN+ TCs analyzed that merge with sorting endosomes within 10 minutes of MST-HN addition, all have associated APPL1. For example, Fig. 2B (supplementary material Movie 4) shows data obtained using a two plane MUM configuration. In the early stages of the movie

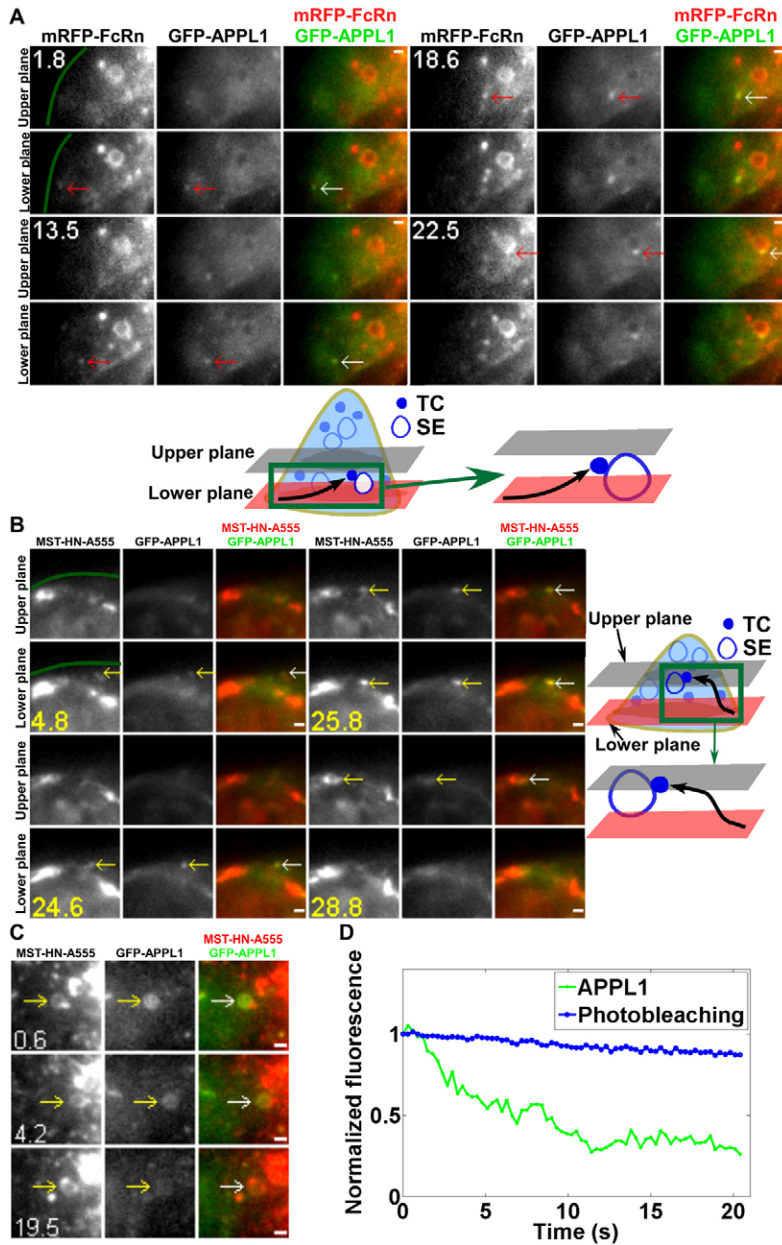


Fig. 2. APPL1+ TCs are involved in a pre-endosomal sorting step. HMEC-1 cells were cotransfected with mRFP-FcRn/ β_2 m/GFP-APPL1 (A) or FcRn-stop/ β_2 m/GFP-APPL1 (B,C).

Transfected cells were incubated with Alexa 555-MST-HN for 2 min before imaging (B,C). White (or colored) arrows in the overlay (or single color) images show the events or regions of interest. Scale bars: 1 μ m. Green lines in A and B demarcate the plasma membrane. Images show selected frames from a dataset continuously acquired at a frame rate of 3 frames per second.

(A) Selected frames from supplementary material Movie 3. A GFP-APPL1+mRFP-FcRn+ TC appears near the edge of the cell (1.8 s), moves between the two focal planes and merges with a sorting endosome (SE) (22.5 s) (shown schematically below).

(B) Selected frames from supplementary material Movie 4. An APPL1+MST-HN+ TC appears in the lower plane (4.8 s), moves to the upper plane (25.8 s) and merges with a sorting endosome (28.8 s) (shown schematically on the right).

(C) An APPL1+MST-HN+ sorting endosome loses GFP-APPL1 fluorescence over \sim 20 s. (D) The average photobleaching rate of GFP-APPL1 signal in the same cell is lower than the rate of decrease of GFP-APPL1 signal in the sorting endosome shown in C.

(4.8–25.8 s), an MST-HN+APPL1+ TC can be clearly seen. This TC migrates from the lower plane to the upper plane (25.8 s) and subsequently fuses with a sorting endosome. Collectively, the data demonstrate that APPL1 is associated with FcRn+ TCs preceding endosomal fusion and sorting. Significantly, FcRn association with APPL1+ TCs is observed in HMEC-1 cells following incubation with wild-type human IgG1 (supplementary material Fig. S1), demonstrating that the presence of FcRn in these compartments is not due to treatment of cells with the MST-HN variant.

APPL1 is undetectable or rapidly lost from sorting endosomes following TC fusion

Although APPL1+ TCs fuse with sorting endosomes (Fig. 2A,B), we could not detect APPL1 on the majority of these ‘acceptor’ compartments. This suggests that APPL1 is lost during fusion

events involving APPL1+ TCs, although we cannot exclude the possibility that the APPL1 signal becomes undetectable due to diffusion from the TC into the larger surface area of a sorting endosome following fusion. In rare cases (3 of 36 sorting endosomes analyzed) when APPL1 is detectable on the sorting endosome, the signal intensity decreases more rapidly than the photobleaching rate (Fig. 2C,D). APPL1 therefore dissociates from sorting endosomes, consistent with earlier studies indicating that this protein is displaced by EEA1 through competition for binding to Rab5 (Zoncu et al., 2009).

Analyses of the distribution of SNX4, Rab4 and Rab11 in sorting endosomes and TCs

In previous studies SNX4, Rab4 and Rab11 have been associated with endosomal sorting and recycling (Sönnichsen et al., 2000; McCaffrey et al., 2001; Pagano et al., 2004; Traer et al., 2007).

Towards analyzing the trafficking pathways of TCs following their segregation from sorting endosomes, we next investigated the distribution of these proteins in sorting endosomes and TCs. On endosomes and TCs, SNX4 and Rab4 are almost completely colocalized. For a total of 187 SNX4+ or Rab4+ TCs analyzed, $96 \pm 4\%$ are positive for both SNX4 and Rab4 (Fig. 3A). By contrast, Rab11 is less extensively colocalized with SNX4 or Rab4 in TCs (Fig. 3B), although SNX4, Rab4 and Rab11 are present on all sorting endosomes.

SNX4, Rab4 and Rab11 can associate with APPL1+ TCs

Analyses of the distribution of SNX4 on TCs led to the unexpected observation that this sorting nexin can be present at the pre-endosomal sorting step involving APPL1+ TCs. Specifically, analyses of HMEC-1 cells transfected with GFP-APPL1, mCherry-SNX4 and FcRn-stop followed by pulsing with Atto 647-labeled IgG1 mutant, MST-HN (Vaccaro et al., 2005), indicated that $56 \pm 5\%$ (of 195 TCs analyzed) of APPL1+MST-HN+ TCs have associated SNX4 (Fig. 3C). Further, live cell imaging of HMEC-1 cells transfected with mCherry-SNX4 and GFP-APPL1 demonstrated that APPL1+SNX4+ TCs fuse with sorting endosomes (Fig. 3D). Of a total of seven APPL1+ TCs analyzed that fuse with sorting endosomes, all have detectable levels of SNX4 (Fig. 3D), suggesting that the presence of SNX4 is a marker of fusion competent TCs.

Consistent with the observation that SNX4 is associated with a subset of APPL1+ TCs and extensively colocalized with Rab4 (Fig. 3A), staining of GFP-FcRn/mRFP-Rab4 transfected cells with a polyclonal antibody specific for APPL1 and APPL2 demonstrated that $53 \pm 3\%$ (of a total of 257 FcRn+APPL+ TCs analyzed) of FcRn+APPL+ TCs are also Rab4+ (Fig. 3E). In addition, we investigated whether Rab11, which is associated with endosomal sorting on the exocytic pathway in HMEC-1 cells (Ward et al., 2005), colocalizes with APPL. To assess overlap between APPL and Rab11, HMEC-1 cells were transfected with GFP-Rab11 and stained with anti-APPL antibody following fixation. Since we hypothesized that SNX4 is a marker of fusion competent TCs, cells were co-transfected with mCherry-SNX4 for these analyses. To enable localization of FcRn by pulsing with labeled MST-HN, cells were also co-transfected with FcRn-stop (Fig. 3F). A relatively low proportion ($9 \pm 2\%$ of 253 TCs analyzed) of FcRn+APPL+ TCs have associated SNX4 and Rab11. Further, $43 \pm 3\%$ of APPL+FcRn+ TCs have associated SNX4 (with no detectable Rab11), whereas $13 \pm 2\%$ of APPL+FcRn+ TCs have associated Rab11 (with no detectable SNX4). Thus, SNX4, Rab4 and Rab11 can unexpectedly associate with APPL+FcRn+ TCs at the pre-endosomal sorting stage of the recycling pathway, although SNX4 or Rab4 association is more common than that of Rab11. Collectively, pre-endosomal TCs have associated APPL, with the possible presence of SNX4, Rab4 and Rab11 for partially overlapping subsets of these TCs (Fig. 3G). Importantly, the colocalization of APPL with Rab4, Rab11 and SNX4 is similar in FcRn-stop transfected cells treated with wild-type IgG or MST-HN mutant (supplementary material Fig. S2), indicating that treatment of cells with MST-HN does not perturb the behavior of APPL+ TCs.

Interendosomal transfer TCs have associated SNX4 and Rab4 without detectable levels of APPL1 or Rab11

Whilst analyzing APPL1 associations with TCs, we also observed endosomal fusion of FcRn+ TCs without detectable levels of

APPL1. Collectively with our earlier observations that TCs can migrate between endosomes (Ober et al., 2004b), this prompted us to further analyze these interendosomal transfer events. Given the previously identified role of SNX4 in endosomal sorting (Traer et al., 2007; Cullen, 2008), we first investigated whether TCs involved in interendosomal transfer have associated SNX4 by co-transfecting HMEC-1 cells with GFP-SNX4 and mRFP-FcRn. SNX4+FcRn+ TCs can fuse with other sorting endosomes of similar size and morphology (a total of five merging SNX4+FcRn+ TCs was observed). In Fig. 4A (supplementary material Movie 5), a representative event of this type is shown. A SNX4+FcRn+ TC leaves a sorting endosome in the upper plane, migrates to the lower plane (6 s) and fuses with a second endosome. By contrast with SNX4, the analysis of cells co-transfected with GFP-Rab11 and mCherry-SNX4 indicated that Rab11 does not associate with interendosomal TCs (a total of 11 interendosomal SNX4+Rab11- TCs was observed). In the example shown (Fig. 4B), a SNX4+ TC leaves a sorting endosome and moves in the same plane to fuse with a second sorting endosome.

Consistent with the extensive colocalization of Rab4 and SNX4 (Fig. 3A), we also observed interendosomal transfer events involving SNX4+Rab4+ TCs in cells transfected with PAGFP-Rab4 and mCherry-SNX4 followed by local photoactivation of PAGFP-Rab4 on individual sorting endosomes (a total of nine interendosomal SNX4+Rab4+ TCs was observed). In Fig. 5A, a SNX4+Rab4+ TC leaves a sorting endosome and fuses with a proximal sorting endosome within the same focal plane. A second TC also leaves this endosome in the lower focal plane, moves to the upper focal plane (64.5 s), migrates back and forth (66.6 s) and returns to fuse with the second endosome (Fig. 5B; supplementary material Movie 6).

LP-MUM experiments using transfectants expressing FcRn-PAGFP and mRFP-Rab4 resulted in the observation of transfer of Rab4+FcRn+ TCs between two sorting endosomes that were photoactivated sequentially (Fig. 5C). In addition, when multiple interendosomal transfer events occurred from an individual sorting endosome (four different endosomes, two transfer events per endosome), transfer was unidirectional, suggesting that the donor endosomes may be upstream of the acceptor endosomes on the recycling pathway. Despite the presence of Rab11 on donor and acceptor endosomes, the migrating TCs do not have detectable levels of Rab11 (total of 15 interendosomal transfer TCs analyzed; Fig. 4B). Consistent with current and earlier studies of APPL1 (Miaczynska et al., 2004; Zoncu et al., 2009), these TCs also do not have associated APPL1 (total of five interendosomal transfer TCs analyzed). Interendosomal transfer TCs are therefore SNX4+Rab4+, with undetectable levels of Rab11 and APPL1.

TCs involved in looping events are associated with both SNX4/Rab4 and Rab11

A novel class of looping events involving the segregation of TCs from sorting endosomes and their subsequent return to the same endosome was observed in cells transfected with different combinations of Rab4, Rab11, SNX4 and FcRn (PAGFP-Rab11/mCherry-SNX4, FcRn-PAGFP/mRFP-Rab4, FcRn-PAGFP/mCherry-SNX4, mRFP-FcRn/PAGFP-Rab11 or PAGFP-Rab4/mCherry-SNX4; $n=19$ looping events for all transfection combinations). Representative examples of these processes, obtained using LP-MUM, are shown in Fig. 1D, Fig. 6A

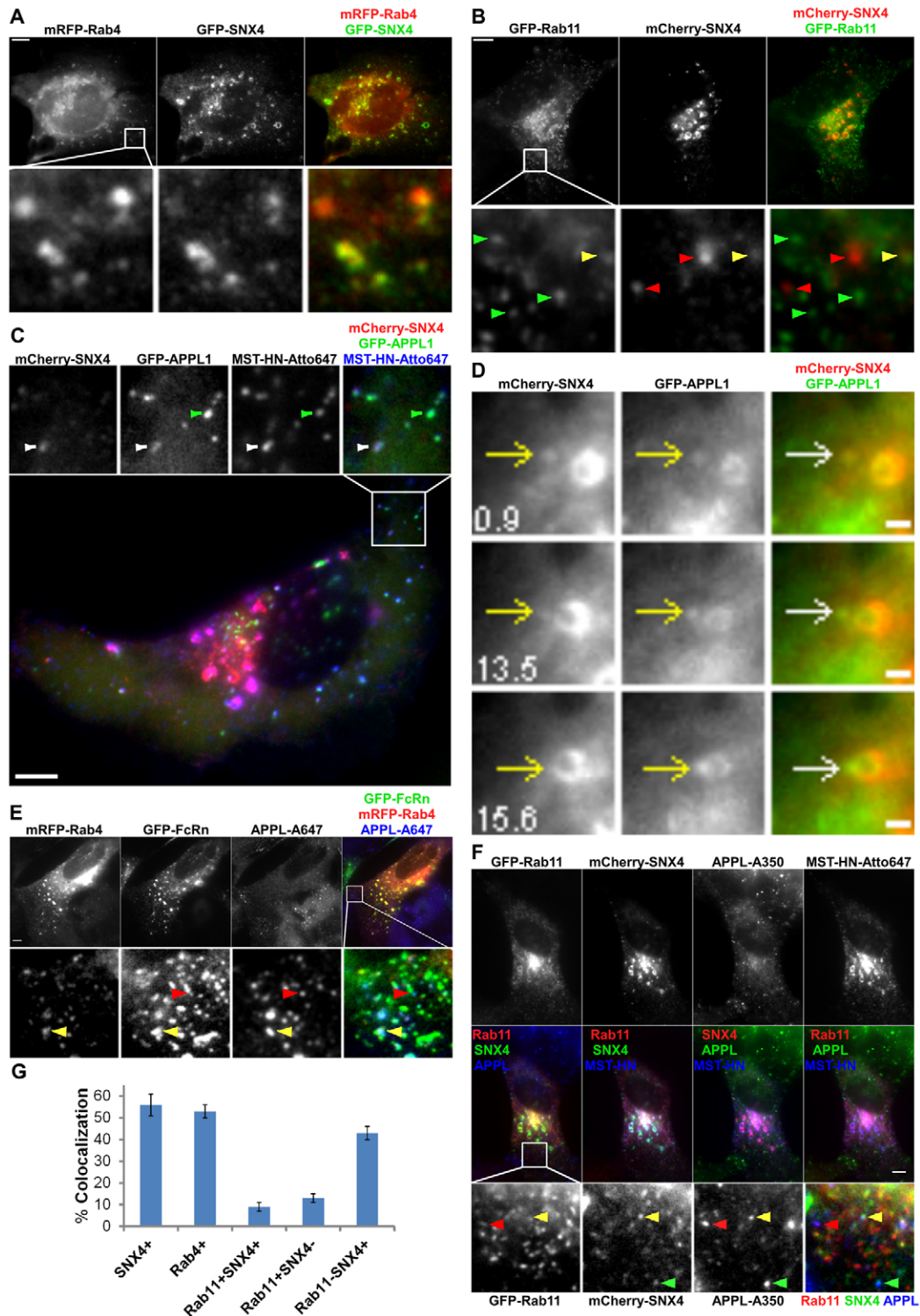


Fig. 3. Analyses of the distribution of SNX4, Rab4 and Rab11 in sorting endosomes and TCs. HMEC-1 cells were cotransfected with GFP-SNX4/mRFP-Rab4 (A), GFP-Rab11/mCherry-SNX4 (B), FcRn-stop/ β_2 m/mCherry-SNX4/GFP-APPL1 (C), mCherry-SNX4/GFP-APPL1 (D), GFP-FcRn/mRFP-Rab4 (E) or FcRn-stop/ β_2 m/GFP-Rab11/mCherry-SNX4 (F). Scale bars: 5 μ m (A-C,E,F) or 1 μ m (D). Transfected cells were fixed (A,B,E), or pulsed with Atto 647-labeled MST-HN for 30 min prior to washing and fixation (C,F). For E and F, cells were stained with anti-APPL antibody. Boxed regions in the upper (A,B,E), lower (C) or middle rows (F) are presented as cropped images in the lower (A,B,E,F) or upper (C) rows. (A) Rab4 and SNX4 colocalize extensively with each other. (B) Red, green or yellow arrowheads indicate examples of SNX4+, Rab11+ or SNX4+Rab11+ TCs, respectively. (C) Green or white arrowheads indicate examples of a MST-HN+APPL1+SNX4- or MST-HN+APPL1+SNX4+ TC, respectively. (D) Images show selected frames from a dataset continuously acquired at a frame rate of 3 frames per second. A SNX4+APPL1+ TC merges with a SNX4+APPL1+ sorting endosome (15.6 s). (E) Yellow or red arrowheads indicate examples of an FcRn+APPL+Rab4+ or FcRn+APPL+Rab4- TC, respectively. (F) The upper (or middle) row shows the single color (or overlay) data. Red, green or yellow arrowheads indicate examples of MST-HN+ TCs that are APPL+Rab11+, APPL+SNX4+ or APPL+SNX4+Rab11+, respectively. (G) Histogram showing percentages of colocalization of Rab4, Rab11 and/or SNX4 with APPL+FcRn+ TCs for the data presented in C, E and F.

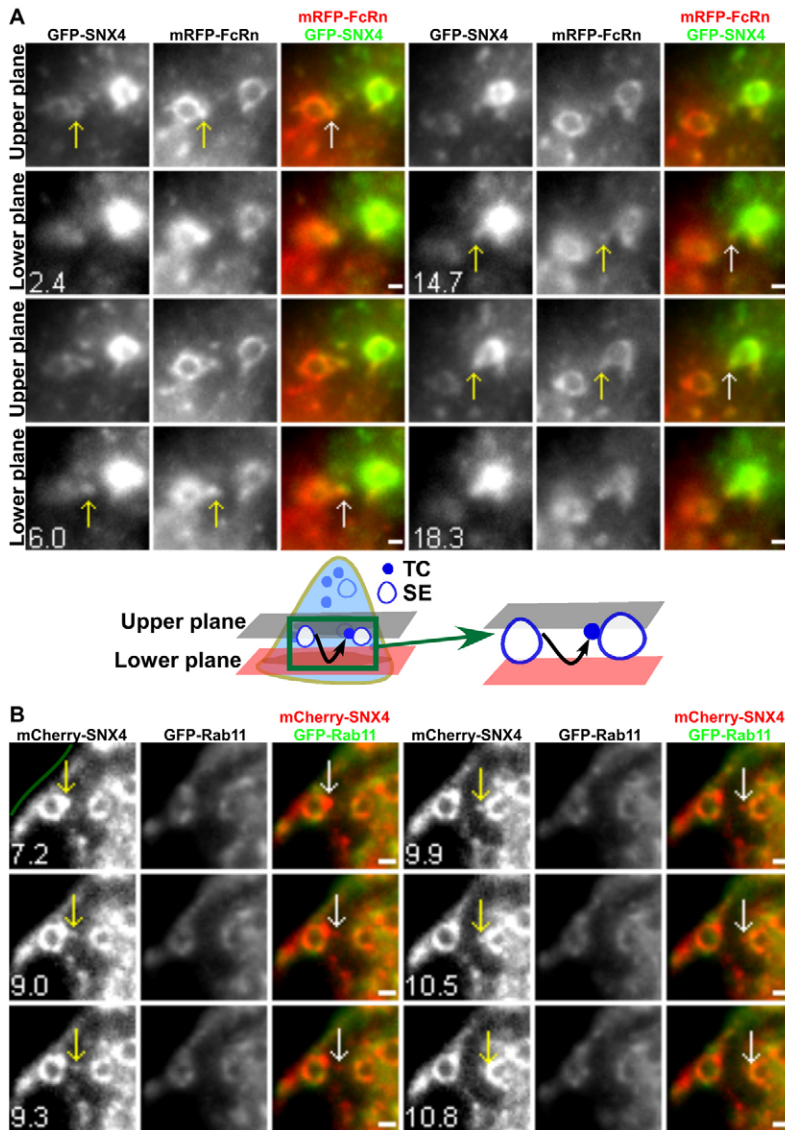


Fig. 4. Interendosomal transfer TCs have associated SNX4 but not Rab11. HMEC-1 cells were cotransfected with GFP-SNX4/ β_2 m/mRFP-FcRn (A) or mCherry-SNX4/GFP-Rab11 (B). Scale bars: 1 μ m. The green line in B demarcates the plasma membrane. Images show selected frames from a dataset continuously acquired at a frame rate of 3 frames per second. (A) Selected frames from supplementary material Movie 5. An FcRn+SNX4+ TC extends from a sorting endosome (SE) (2.4–6.0 s), segregates and moves between the two focal planes. This TC merges with another sorting endosome (18.3 s) (shown schematically below). (B) A SNX4+Rab11– TC extends from a sorting endosome (7.2–9.0 s), segregates and subsequently merges with another sorting endosome (10.5 s).

(supplementary material Movie 7) and Fig. 6B (supplementary material Movie 8). Although the Rab11-associated fluorescence is very high in a tubule extending from the sorting endosome in Fig. 6B, lower levels of Rab11 can still be detected on the limiting membrane of the endosome. This is consistent with earlier reports (Sönnichsen et al., 2000; Ward et al., 2005) demonstrating that Rab GTPases can localize to discrete domains on endosomes. Looping events are frequently of relatively long duration, accounting for their difficulty in detection in earlier studies using conventional imaging modalities. The TCs segregate from the endosome, pause and then reverse direction to return and fuse with the originating endosome. In 17 of 19 looping events analyzed, the TC moves towards the cell periphery before reversing direction. Further, in PAGFP-Rab11/mCherry-SNX4 transfected cells, all of a total of 6 looping TCs analyzed have associated Rab11 and SNX4, indicating that looping TCs can be distinguished from interendosomal transfer TCs by the presence of Rab11.

Although for technical reasons it was not possible to track looping events in APPL1-GFP transfected cells, several observations indicate that APPL1 is not present on looping

TCs. First, in GFP-APPL1 transfected cells, APPL1 is not associated with any TCs that segregate from sorting endosomes, consistent with the low or undetectable levels of APPL1 on these endosomes. Second, in GFP-APPL1 transfected cells pulsed with MST-HN for short periods to label the early stages in endocytic recycling, the majority ($89 \pm 3\%$ of a total of 119 TCs analyzed) of APPL1+ TCs have associated MST-HN, suggesting that APPL1 is predominantly associated with pre-endosomal TCs. Further, the low percentage ($11 \pm 3\%$) of APPL1+ TCs that do not contain MST-HN are also SNX4–.

Post-endosomal sorting TCs are associated with Rab11 without detectable levels of SNX4 or Rab4

In experiments with SNX4 or Rab4 transfected cells, a subset of FcRn+ TCs segregate from sorting endosomes that are not involved in interendosomal transfer or looping events. These TCs do not contain detectable levels of SNX4 or Rab4 (of a total of four SNX4– and three Rab4– TCs). Collectively with our earlier observations that Rab11 is associated with exocytic events involving FcRn (Ward et al., 2005), this suggested that such TCs

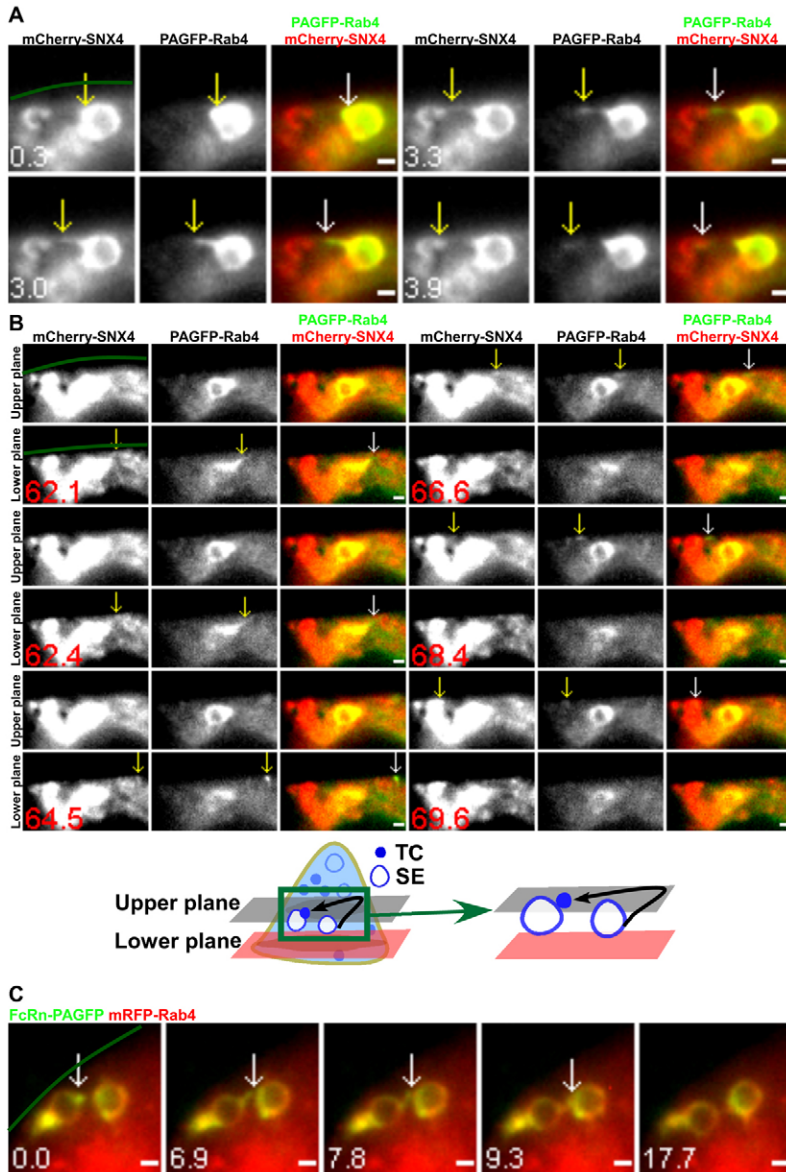


Fig. 5. Interendosomal transfer TCs have associated SNX4/Rab4. HMEC-1 cells were cotransfected with mCherry-SNX4/PAGFP-Rab4 (**A,B**) or mRFP-Rab4/ β_2m /FcRn-PAGFP (**C**). PAGFP in individual sorting endosomes (SEs) was photoactivated. Scale bars: 1 μ m. Green lines demarcate the plasma membrane. Images show selected frames from a dataset continuously acquired at a frame rate of 3 frames per second. (**A**) A SNX4+Rab4+ TC extends from a sorting endosome (0.3–3.3 s), segregates and subsequently merges with another sorting endosome (3.9 s). (**B**) Selected frames from supplementary material Movie 6. A second SNX4+Rab4+ TC leaves the same ‘donor’ sorting endosome as in **A** in the lower plane (62.1 s), moves rightwards at 64.5 s, changes direction and moves leftwards at 66.6 s. It merges with the ‘acceptor’ sorting endosome in the upper plane (69.6 s) (shown schematically below). (**C**) Two Rab4+ sorting endosomes were photoactivated sequentially. A FcRn+Rab4+ TC extends from one sorting endosome at 0 s, merges with the second sorting endosome (6.9–7.8 s) and subsequently segregates from the original endosome.

might be on the post-endosomal sorting pathway leading to exocytosis. LP-MUM proved to be essential for the analysis of the behavior of Rab11+ TCs due to the high background haze of Rab11-associated fluorescence. By contrast with the properties of Rab4+ TCs, imaging of cells following co-transfection with PAGFP-Rab11 and mRFP-FcRn resulted in the observation of Rab11+FcRn+ TCs leaving sorting endosomes and frequently moving to the cell periphery (Fig. 7A; supplementary material Movie 9). In Fig. 7A, the TC moves from the upper plane to the lower plane and disappears from the field of view (i.e. moves towards the plasma membrane which is juxtaposed to the coverglass). Similarly, in mCherry-SNX4/PAGFP-Rab11 transfected cells, Rab11+ TCs with undetectable levels of SNX4 can be seen leaving endosomes, migrating from the upper plane towards the cell periphery in the lower plane before being lost from the field of view (7.2–26.4 s) (Fig. 7B; supplementary material Movie 10). Within the time frame of imaging, none of these Rab11+FcRn+ TCs (total of five analyzed) or Rab11+SNX4- TCs (total of six analyzed) are

involved in interendosomal transfer or looping events. Instead, the TCs migrate towards the plasma membrane. Collectively, Rab11, but not SNX4 or Rab4, is associated with post-endosomal sorting TCs. Combined with our earlier TIRFM analyses (Ward et al., 2005), these TCs most likely lead to exocytosis of FcRn.

We have previously used TIRFM to demonstrate that, by contrast with Rab11, Rab4 is not associated with exocytic events (Ward et al., 2005). The extensive colocalization of Rab4 and SNX4 with each other (Fig. 3A) indicated that SNX4 would also not be associated with exocytic processes. This was confirmed by TIRFM analyses of HMEC-1 cells co-transfected with mCherry-SNX4 and GFP-FcRn. In all of a total of 14 exocytic events involving FcRn, we could not detect SNX4 (supplementary material Fig. S3A). Analogous analyses of cells co-transfected with mRFP-APPL1 and FcRn tagged with ecliptic pHluorin (Prabhat et al., 2007) demonstrated that exocytic events involving FcRn do not have detectable levels of APPL1 (supplementary material Fig. S3B).

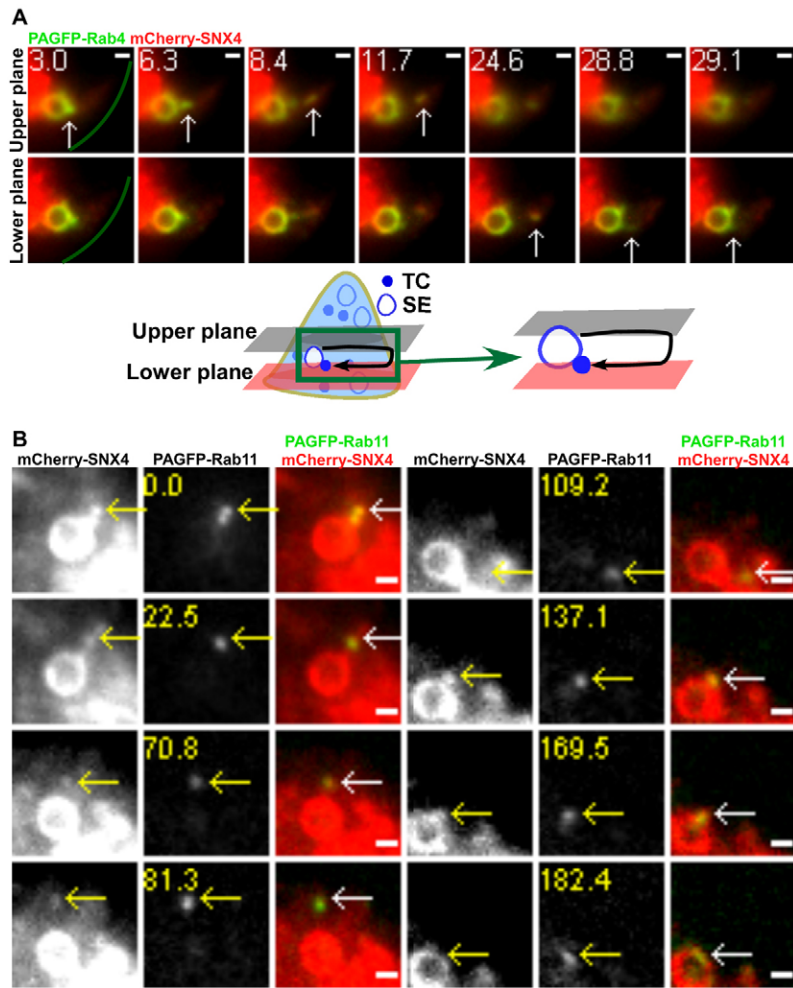


Fig. 6. TCs involved in looping events have associated SNX4/Rab4 and Rab11. HMEC-1 cells were cotransfected with PAGFP-Rab4/mCherry-SNX4 (A) or mCherry-SNX4/PAGFP-Rab11 (B). PAGFP in individual sorting endosomes (SEs) was photoactivated. Scale bars: 1 μ m. Green lines in A demarcate the plasma membrane. Images show selected frames from a dataset continuously acquired at a frame rate of 3 frames per second. (A) Selected frames from supplementary material Movie 7. A SNX4+Rab4+ TC extends from a sorting endosome (3–6.3 s) in the upper plane, segregates and subsequently moves to the lower plane at 24.6 s. This TC returns and merges with the same endosome (29.1 s) (shown schematically below). (B) Selected frames from supplementary material Movie 8. A SNX4+Rab11+ TC extends from a sorting endosome (0 s), segregates and subsequently returns and merges with the same endosome (137.1–182.4 s).

The pathways taken by TCs are identifiable based on associations with APPL1, SNX4, Rab4 and Rab11

Collectively, our results indicate that pre-endosomal TCs can be distinguished from TCs participating later in the endosomal sorting pathway by the presence of APPL1. TCs involved in interendosomal transfer have associated SNX4, Rab4, but no Rab11, whereas looping TCs have all three proteins. By contrast, TCs on the post-endosomal sorting pathway are characterized by the presence of Rab11 without detectable levels of SNX4 or Rab4.

Discussion

Receptor recycling represents an essential component of normal cell physiology. This pathway also provides multiple opportunities for drug targeting and delivery. However, despite extensive analyses, there is a limited understanding concerning recycling processes. A major barrier to the definition of the components constituting this pathway has been the difficulty in characterizing tubulovesicular TCs. Specifically, the itineraries taken by TCs and how their protein associations demarcate TCs at different trafficking steps have to date been elusive. The analysis of TCs is complicated by their formation of a complex, highly dynamic interconnected network within cells. Although significant advances have recently been made in fluorescence microscopy, it has proved extremely challenging to track these

TCs at high spatial and temporal resolution in three dimensions. In the present study we have applied MUM (Prabhat et al., 2004; Prabhat et al., 2007; Ram et al., 2008), combined with localized photoactivation, to overcome these limitations. This has enabled the characterization of the pathways and protein associations of the TCs that participate in the intracellular recycling pathway involving the Fc receptor, FcRn. Such studies not only have relevance to understanding the recycling process for which FcRn is a representative receptor, but also provide a framework for global analyses of TCs in cells.

Our studies have resulted in the identification of several discrete pathway components that involve TCs and constitute recycling. Importantly, the TCs participating in these components can be distinguished from each other based on associations with the different proteins, APPL1, Rab4 and Rab11 (Fig. 8). The pre-endosomal sorting step involves APPL1+ TCs that fuse with endosomes prior to subsequent trafficking steps. These TCs can also have associated Rab4 and/or Rab11. Following the fusion of APPL1+ TCs with sorting endosomes, the recycling pathway can be categorized into interendosomal transfer, looping or post-endosomal sorting processes. These three possible components are distinguishable based on the following Rab4/Rab11 associations: TCs involved in interendosomal transfer are Rab4+ without detectable levels of Rab11, whereas Rab4+Rab11+ TCs traffick to and from the same sorting endosome in looping events. By contrast

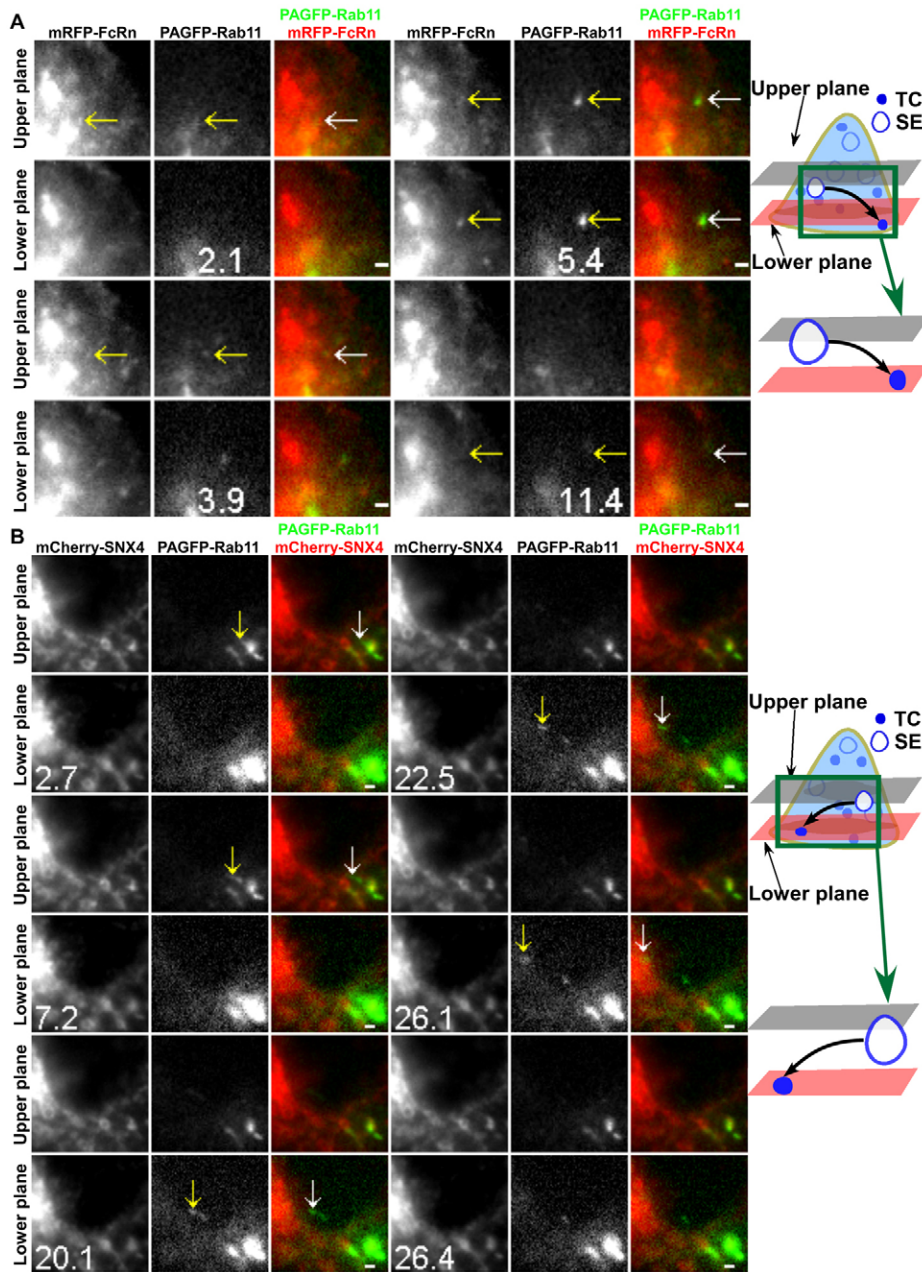


Fig. 7. Post-endosomal sorting TCs are associated with Rab11 without detectable levels of SNX4. HMEC-1 cells were cotransfected with mRFP-FcRn/ β_2m /PAGFP-Rab11 (A) or PAGFP-Rab11/mCherry-SNX4 (B). A 405 nm laser beam was focused onto an FcRn+ (A) or SNX4+ (B) sorting endosome (SE) for ~ 1 s to photoactivate PAGFP (associated with Rab11). Individual images are presented with the time (in seconds) at which each image was acquired (the first image is arbitrarily set to time 0). White arrows in the overlay images show the events of interest that are also indicated in the single color data by yellow arrows. Schematic representations are shown in the right-hand column. Scale bars: 1 μ m. Images show selected frames from a dataset continuously acquired at a frame rate of 3 frames per second. (A) Selected frames from supplementary material Movie 9. A FcRn+Rab11+ TC extends from a sorting endosome (2.1 s), segregates and subsequently moves to the lower plane (5.4 s). This TC disappears from the lower plane (11.4 s). (B) Selected frames from supplementary material Movie 10. A SNX4-Rab11+ TC extends from a sorting endosome (2.7 s), segregates and subsequently moves to the lower plane (20.1 s). This TC disappears from the lower plane (26.4 s).

with the pathways involving transport to and from endosomes, the post-endosomal sorting component of recycling is characterized by the segregation of Rab11+ (Rab4⁻) TCs from sorting endosomes followed by their migration to the cell periphery. We also observe that the majority of SNX4+ TCs have associated Rab4.

At the pre-endosomal sorting step, APPL1 can be used as a marker of FcRn+ TCs that fuse with sorting endosomes. In earlier studies, APPL1+ endosomes and macropinosomes have been shown to transport signaling receptors within cells following internalization by clathrin or non-clathrin-mediated pathways (Miaczynska et al., 2004; Zoncu et al., 2009). In the present study we extend the role of APPL1+ TCs to the transport of receptors that have no known signaling activity. Consistent with earlier studies showing that EEA1 competes for APPL1 binding to Rab5 (Zoncu et al., 2009), in the present study APPL1 is either undetectable or rapidly lost from larger EEA1+ sorting endosomes.

Interestingly, SNX4 can also be associated with a subset of APPL1+ TCs. This is unexpected since earlier studies demonstrated that SNX4 is involved in the tubulation of sorting endosomes followed by transport of SNX4+ TCs to recycling endosomes (Traer et al., 2007), rather than the pre-endosomal sorting step. Significantly, all fusion events of APPL1+ TCs with sorting endosomes have associated SNX4, suggesting that this protein accumulates on the TCs as they mature. Rab4, which is extensively colocalized with SNX4, is also present on a subset ($\sim 50\%$) of APPL1+ TCs. A relatively small proportion ($9 \pm 2\%$) of APPL1+ TCs have detectable levels of both SNX4 and Rab11. Thus, although TCs that fuse with endosomes prior to endosomal sorting can be uniquely identified by the presence of APPL1, these TCs can also have associated SNX4, Rab4 and/or Rab11.

A longstanding question in cell biology is how do early/sorting endosomes form? Models involving the delivery of internalizing

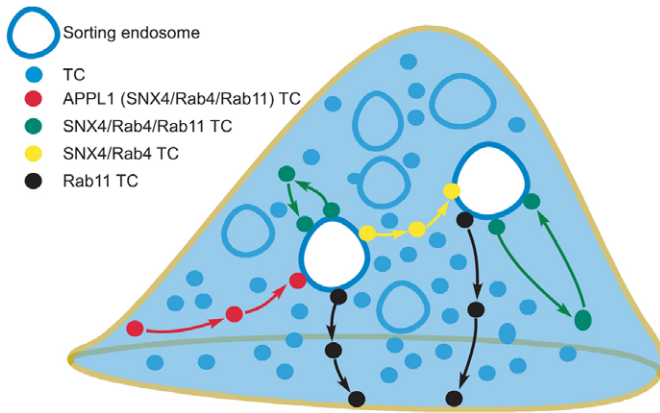


Fig. 8. Schematic representation of the routes taken by TCs in the recycling pathway. The model shows pre-endosomal sorting TCs (APPL1+, that can also have associated SNX4, Rab4 and/or Rab11), post-endosomal sorting TCs (Rab11+), interendosomal transfer TCs (SNX4+Rab4+) or looping TCs (SNX4+Rab4+Rab11+).

receptors via vesicular transport to sorting endosomes (Griffiths and Gruenberg, 1991; Zerial and McBride, 2001) have recently been challenged by the observation of homotypic fusion of incoming vesicles followed by their maturation to generate larger early/sorting endosomes (Zoncu et al., 2009). In another study (Rink et al., 2005), the early to late endosome transition involves a maturation process designated Rab conversion that also includes homotypic fusion of early endosomes (Helenius et al., 1983; Murphy, 1991). In the present study we show that APPL1+ TCs formed early on the endocytic pathway fuse with larger, more static sorting endosomes, indicating vesicular transport in this component of the endosomal recycling pathway. Collectively, it is likely that both vesicular transport and maturation models are relevant to endosomal pathways (Rink et al., 2005).

The presence of SNX4 and Rab4 on interendosomal transfer, looping TCs and fusing APPL1+ TCs suggests that these proteins mark TCs 'competent' to fuse with either the same or other sorting endosomes. Prior reports demonstrating Rab4–syntaxin 4 or 13 associations (Li et al., 2001; Hoogenraad et al., 2010) indicate that these SNARE proteins could be involved in fusion with sorting endosomes. In support of this concept, post-endosomal sorting Rab11+ TCs do not have detectable levels of SNX4 or Rab4 and leave sorting endosomes prior to fusion with the plasma membrane.

The question arises concerning the function of looping events involving the apparently futile cycling of TCs to and from the same endosome? These events could represent erroneous sorting steps that require subsequent editing by addition/removal of proteins following return to the parent endosome. Such processes could be analogous to enzymatic proofreading and improve the fidelity of trafficking. Related to this, looping TCs may contain unliganded FcRn that is returned to the same endosome to enable interactions with incoming IgG.

Looping TCs could accumulate other, as yet undefined, protein(s) as they migrate through the cytosol, resulting in a change in composition of the parent endosome. This could also account for the frequent pauses and turnarounds that are observed for nearly all of these TCs. The relatively long pauses by looping

TCs may also be due to interactions with other (unlabeled) compartments. Although we cannot exclude the possibility that these TCs undergo kiss-and-linger type interactions (Holroyd et al., 2002; Taraska et al., 2003; Tsuboi and Rutter, 2003) with these compartments, they do not merge. The behavior of looping TCs suggests the involvement of different motor proteins such as kinesins and dyneins that oppose each other's motion (Schuster et al., 2011). These motor proteins are associated with movement on microtubules in the minus end direction towards the center of the cell (dynein) or plus end direction towards the cell periphery (kinesin) (Schuster et al., 2011). Both Rab4 and Rab11 can associate with dynein and/or kinesin (Bielli et al., 2001; Imamura et al., 2003; Schonteich et al., 2008; Horgan et al., 2010), and SNX4 has been shown to bind to dynein indirectly through KIBRA (Traer et al., 2007). It is therefore tempting to speculate that SNX4+Rab4+Rab11+ looping TCs initially move towards the cell periphery due to a dominance of kinesin-directed motion, followed by dynein loading resulting from an increase in dynein concentration towards the cell periphery (Schuster et al., 2011). This could result in retrograde, minus end-directed motion towards the donor endosome (Schuster et al., 2011; Yao et al., 2012).

Our analyses are consistent with the previously ascribed roles of Rab4 and Rab11 in the regulation of receptor recycling (van der Sluijs et al., 1992; Ullrich et al., 1996; McCaffrey et al., 2001; Pagano et al., 2004; Schonteich et al., 2008). In both our current and earlier analyses, Rab11 is associated with post-endosomal TCs that directly recycle from sorting endosomes to the plasma membrane (Ward et al., 2005). By contrast, SNX4/Rab4+ TCs (with or without associated Rab11) migrate to other, or even the same, sorting endosomes in cells. Although Rab4 has been associated with fast recycling (van der Sluijs et al., 1992; Sönnichsen et al., 2000), the current studies indicate a distinct role, primarily involving inter- or intra-endosomal transfer events. These observations are also consistent with earlier analyses demonstrating that Rab4 is not associated with exocytic events (Ward et al., 2005).

The model shown in Fig. 8 describes pathway components involved in recycling which forms a basis for further analyses. For example, the connectivity between the different steps to form a complete recycling circuit for FcRn (or any receptor) remains uncertain. For example, does cargo in all TCs undergo interendosomal transfer and/or looping before being sorted into TCs destined for exocytosis? Can a recycling receptor undergo multiple interendosomal transfer events? These questions also relate to defining the trafficking components that constitute the fast and slow recycling pathways (Hopkins and Trowbridge, 1983; Sheff et al., 1999; Maxfield and McGraw, 2004; Grant and Donaldson, 2009). For example, looping and interendosomal transfer events could contribute to slow recycling. To address these issues, it will be necessary to carry out single molecule tracking studies for complete cycles of the recycling pathway in three dimensions, which has to date not been achieved due to the enormous technical challenges that such analyses present.

In summary, we have characterized the spatiotemporal dynamics of the TCs involved in different steps of the recycling pathway of FcRn. Importantly, the current study has resulted in the identification of different combinations of APPL1, SNX4, Rab4 and Rab11 on tubulovesicular TCs as markers of distinct trafficking components. Incoming APPL1+ TCs fuse with more static sorting endosomes, providing support for

vesicular transport models in this early part of the recycling pathway. Our data also reveal a novel process involving looping TCs that migrate to and from the same endosome. Finally, we expect that the observations and approaches used in the present study could have relevance to multiple other receptors and cargo on endolysosomal/recycling pathways.

Materials and Methods

Plasmid constructs

GFP-Rab4 and GFP-Rab11 constructs were generously provided by M. Zerial (Max Planck Institute of Molecular Cell Biology and Genetics, Germany). GFP-SNX4 (human) and mCherry-SNX4 (human) constructs were a generous gift of P. Cullen (University of Bristol, UK). The mRFP gene (Campbell et al., 2002) was generously provided by R. Tsien (UCSD, CA). PAGFP-C1 and PAGFP-N1 constructs were generously provided by G. Patterson (NIBIB). GFP-APPL1 and mRFP-APPL1 constructs (Zoncu et al., 2009) were purchased from Addgene (Cambridge, MA). FcRn-GFP, GFP-FcRn, mRFP-FcRn, pFluorin-FcRn and human β_2 -microglobulin (β_2m) constructs have been described previously (Ober et al., 2004b; Ward et al., 2005; Prabhat et al., 2007; Gan et al., 2009).

All FcRn and FcRn-fluorescent protein constructs used in the present study contained a mutated variant of human FcRn ('79-89/136-147') that has been engineered to have a higher binding affinity for human IgG1 (Vaccaro et al., 2005; Zhou et al., 2005). The FcRn-stop construct was generated by inserting a stop codon between the C terminus of the FcRn gene and GFP in FcRn-GFP and was used in pulsing experiments with labeled IgG1. The FcRn-PAGFP construct was generated by cloning the full length FcRn gene into PAGFP-N1 as an *EcoRI* fragment, as described previously for FcRn-GFP (Ober et al., 2004b). The mRFP-Rab4, mRFP-Rab11, PAGFP-Rab4 and PAGFP-Rab11 constructs were generated by cloning Rab4 and Rab11 genes into mRFP-C1 (Campbell et al., 2002; Gan et al., 2009) or PAGFP-C1 as *KpnI-BamHI* fragments. The PAGFP-SNX4 construct was generated by cloning the SNX4 gene into PAGFP-C1 as a *HindIII-XmaI* fragment.

Antibodies and labeling

Human IgG1 (wild type or MST-HN mutant; Vaccaro et al., 2005) was labeled with Atto 647N-NHS (Atto-Tec, Siegen, Germany), Alexa Fluor 555 or Alexa Fluor 647 (Invitrogen, Carlsbad, CA) using methods recommended by the manufacturer. The degrees of labeling were 5.4 (MST-HN, Alexa 555), 1.3 (MST-HN, Atto 647N), 2.2 (MST-HN, Alexa 647) or 3.3 (wild type, Alexa 647) dye molecules per antibody molecule. The rabbit polyclonal anti-human APPL and mouse monoclonal anti-human EEA1 antibodies were purchased from Abcam (Cambridge, UK) and BD Biosciences (San Jose, CA), respectively.

Transfections

HMEC-1 cells were transiently cotransfected with different combinations of DNA using Nucleofector technology (Amaxa Biosystems, Cologne, Germany) as described previously (Ober et al., 2004b; Ward et al., 2005). The concentrations of DNA used for each fluorescently labeled protein were optimized for each combination and ranged from 0.2–1 μ g. Immediately following transfection, cells were plated on MatTek dishes (MatTek, Ashland, MA) that were custom fitted with round glass coverslips (Electron Microscopy Sciences, Hatfield, PA) and incubated as described previously (Ober et al., 2004b). Cells transfected with FcRn-stop and β_2m were incubated with 5 μ g/mL Atto 647, Alexa Fluor 555 or Alexa Fluor 647-labeled MST-HN or 25/200 μ g/mL Alexa Fluor 647-labeled wild type IgG1 in Phenol Red-free Ham's F-12 K medium at pH \sim 7.4 for various times prior to imaging or fixation.

To ensure that the expression of Rab proteins and SNX4 did not affect the recycling pathway in transfected cells, HMEC-1 cells were co-transfected with different combinations of SNX4 and Rab proteins. Recycling rates of labeled transferrin were analyzed using flow cytometry (Ward et al., 2005). For cells co-expressing Rab proteins and SNX4 at the levels used for imaging, no significant differences in the transferrin recycling rates were observed between transfected and untransfected cells.

Immunofluorescence staining

Cells were fixed using 1.7% (w/v) paraformaldehyde with 0.1% (v/v) glutaraldehyde (10 minutes on ice) and permeabilized using 0.02% (w/v) saponin in phosphate buffered saline (PBS; 10 minutes on ice). Cells were then pre-blocked with 4% BSA/PBS, incubated with primary antibodies in 1% BSA/PBS for 25 minutes at room temperature, and subsequently treated with serum diluted 100-fold from the same host animal in which the secondary antibody was raised. Bound primary antibody was detected by treatment with secondary antibody conjugates for 25 minutes at room temperature. Cells were washed twice with PBS between each incubation, and following the final wash, the cells were immersed in 1.5–2 ml of 1% BSA/PBS containing 0.05% sodium azide.

Fixed cell imaging setup

Images were acquired using a Zeiss Axiovert 200M inverted fluorescence microscope with a Zeiss 1.4 NA 63 \times Plan-apochromat objective and a Hamamatsu Orca 100 CCD camera (Bridgewater, NJ). The cells were imaged with filter sets (Chroma Technologies, Battleboro, VT) that are specific for eGFP (filter set #41017), mRFP/mCherry/Alexa 555 (filter set #41002b), Atto 647N (filter set #41008) and Alexa 350 (custom filter set with exciter-D365/10X, dichroic-380 DCLP and emitter-D460/50m).

LP-MUM configuration

The LP-MUM configuration is based on a dual objective MUM setup (Ram et al., 2009) that was built using two Zeiss microscopes, with one of the microscopes (top scope) mounted in an upside down orientation above the other microscope (bottom scope) (supplementary material Fig. S4). The top scope was equipped with a confocal scan head (DCS120, Becker-Hickl GmbH, Berlin, Germany) and a Zeiss Achroplan 63 \times , 0.95 NA water dipping objective. A 405 nm laser (Becker Hickl GmbH) was fiber optically coupled to the confocal scan head. The bottom scope was equipped with a Zeiss 1.45 NA 100 \times Plan-Fluar oil immersion objective and four high resolution CCD cameras (see below). The cell sample, which was placed in the bottom scope, was illuminated with one or more of the following laser lines through the bottom scope: 488 nm solid state laser (Coherent, Santa Clara, CA) for GFP/PAGFP excitation, 543 nm diode laser (Opto Engine LLC, Midvale, UT) for mRFP/mCherry/Alexa 555 excitation.

The laser lines were reflected from a polychroic mirror (488/543/633 SPC XT) to illuminate the sample. Fluorescence from the cell sample was split by an emission dichroic mirror (560DCSP) into two paths. In the reflected path, mCherry/mRFP fluorescence was passed through an emission filter (HQ605/75) and was split (50:50 beamsplitter) into two CCD cameras (C8484-05G, Hamamatsu, Bridgewater, NJ). In the transmitted path, GFP/PAGFP fluorescence was passed through an emission filter (HQ515/30) and was split (50:50 beamsplitter) into two CCD cameras (iXon DU897, Andor Technologies, South Windsor, CT).

The cell sample was simultaneously imaged in two distinct focal planes. The cameras in the mCherry/mRFP and GFP/PAGFP channels were positioned at specific calibrated distances such that the distance between the two focal planes in the sample was 800 nm. The exposure time for all of the cameras was 0.3 s.

For localized photoactivation of PAGFP, the cell sample was illuminated with the 488 nm and 543 nm lasers and individual endosomes were identified in the mCherry/mRFP channel. The 405 laser was then illuminated on a single endosome for 1 s. Immediately after this, the fluorescence signals from different fluorophores were simultaneously imaged in the two focal planes.

Intensity analyses

All data were processed and displayed using the custom-written MIATool software package (Chao et al., 2010) (www4.utsouthwestern.edu/wardlab) in MATLAB (Mathworks, Natick, MA). The intensities of images from each camera were linearly adjusted to properly display the events of interest. In some cases, different linear intensity adjustments were applied to different time-contiguous segments of images to compensate for photobleaching. Images were overlaid and annotated. In overlay images, the intensities of the individual color channels were adjusted to similar levels.

For intensity analysis of GFP-APPL1 in the sorting endosome in Fig. 2D, the GFP-APPL1+ endosome was manually segmented for each frame. A background intensity value was subtracted from each pixel. The resulting values were added together to obtain the total GFP fluorescence intensities of the compartment in each frame. For photobleaching analysis, a 141 \times 141 region of interest (ROI) within the cell was selected and a background intensity value subtracted from each pixel. The resulting values were added together to obtain the total GFP fluorescence intensities of the ROI in each frame. The total GFP fluorescence intensities of the endosome and ROI were normalized and plotted over time. For core/annulus intensity analyses of exocytic events (supplementary material Fig. S3), methods analogous to those described previously (Prabhat et al., 2007) were used.

To calculate the pairwise colocalization percentages of APPL1, SNX4, Rab4 and Rab11 in TCs, the number of TCs with detectable levels of both proteins of interest was compared with the number of TCs with detectable levels of only one of the two proteins.

Acknowledgements

We thank Alberto Puig-Canto, Siva Devanaboyina and Yen-ching Chao for valuable assistance with this study.

Author contributions

Z.G. performed the experiments, analyzed data and wrote the manuscript; S.R. assisted with the microscope design and data analysis; R.J.O. and E.S.W. designed the experiments and wrote the manuscript.

Funding

This work was supported in part by the National Institutes of Health [grant numbers ROI AI039167, ROI AR056478 and ROI GM085575]; and the National Multiple Sclerosis Society [fellowship number FG 1798 to S.R.]. Deposited in PMC for release after 12 months.

Supplementary material available online at

<http://jcs.biologists.org/lookup/suppl/doi:10.1242/jcs.116327/-DC1>

References

- Antohe, F., Rădulescu, L., Gafencu, A., Gheție, V. and Simionescu, M. (2001). Expression of functionally active FcRn and the differentiated bidirectional transport of IgG in human placental endothelial cells. *Hum. Immunol.* **62**, 93-105.
- Bielli, A., Thörnqvist, P. O., Hendrick, A. G., Finn, R., Fitzgerald, K. and McCaffrey, M. W. (2001). The small GTPase Rab4A interacts with the central region of cytoplasmic dynein light intermediate chain-1. *Biochem. Biophys. Res. Commun.* **281**, 1141-1153.
- Campbell, R. E., Tour, O., Palmer, A. E., Steinbach, P. A., Baird, G. S., Zacharias, D. A. and Tsien, R. Y. (2002). A monomeric red fluorescent protein. *Proc. Natl. Acad. Sci. USA* **99**, 7877-7882.
- Chao, J., Ward, E. S. and Ober, R. J. (2010). A software framework for the analysis of complex microscopy image data. *IEEE Trans. Inf. Technol. Biomed.* **14**, 1075-1087.
- Cullen, P. J. (2008). Endosomal sorting and signalling: an emerging role for sorting nexins. *Nat. Rev. Mol. Cell Biol.* **9**, 574-582.
- Dickinson, B. L., Badizadegan, K., Wu, Z., Ahouse, J. C., Zhu, X., Simister, N. E., Blumberg, R. S. and Lencer, W. I. (1999). Bidirectional FcRn-dependent IgG transport in a polarized human intestinal epithelial cell line. *J. Clin. Invest.* **104**, 903-911.
- Gan, Z., Ram, S., Vaccaro, C., Ober, R. J. and Ward, E. S. (2009). Analyses of the recycling receptor, FcRn, in live cells reveal novel pathways for lysosomal delivery. *Traffic* **10**, 600-614.
- Grant, B. D. and Donaldson, J. G. (2009). Pathways and mechanisms of endocytic recycling. *Nat. Rev. Mol. Cell Biol.* **10**, 597-608.
- Griffiths, G. and Grunberg, J. (1991). The arguments for pre-existing early and late endosomes. *Trends Cell Biol.* **1**, 5-9.
- He, W., Ladinsky, M. S., Huey-Tubman, K. E., Jensen, G. J., McIntosh, J. R. and Björkman, P. J. (2008). FcRn-mediated antibody transport across epithelial cells revealed by electron tomography. *Nature* **455**, 542-546.
- Helenius, A., Mellman, I., Wall, D. A. and Hubbard, A. (1983). Endosomes. *Trends Biochem. Sci.* **8**, 245-250.
- Holroyd, P., Lang, T., Wenzel, D., De Camilli, P. and Jahn, R. (2002). Imaging direct, dynein-dependent recapture of fusing secretory granules on plasma membrane lawns from PC12 cells. *Proc. Natl. Acad. Sci. USA* **99**, 16806-16811.
- Hoogenraad, C. C., Popa, I., Futai, K., Martínez-Sánchez, E., Wulf, P. S., van Vlijmen, T., Dortland, B. R., Oorschot, V., Govers, R., Monti, M. et al. (2010). Neuron specific Rab4 effector GRASP-1 coordinates membrane specialization and maturation of recycling endosomes. *PLoS Biol.* **8**, e1000283.
- Hopkins, C. R. and Trowbridge, I. S. (1983). Internalization and processing of transferrin and the transferrin receptor in human carcinoma A431 cells. *J. Cell Biol.* **97**, 508-521.
- Horgan, C. P., Hanscom, S. R., Jolly, R. S., Futter, C. E. and McCaffrey, M. W. (2010). Rab11-FIP3 links the Rab11 GTPase and cytoplasmic dynein to mediate transport to the endosomal-recycling compartment. *J. Cell Sci.* **123**, 181-191.
- Hutagalung, A. H. and Novick, P. J. (2011). Role of Rab GTPases in membrane traffic and cell physiology. *Physiol. Rev.* **91**, 119-149.
- Imamura, T., Huang, J., Usui, I., Satoh, H., Bever, J. and Olefsky, J. M. (2003). Insulin-induced GLUT4 translocation involves protein kinase C-lambda-mediated functional coupling between Rab4 and the motor protein kinesin. *Mol. Cell Biol.* **23**, 4892-4900.
- Li, L., Omata, W., Kojima, I. and Shibata, H. (2001). Direct interaction of Rab4 with syntaxin 4. *J. Biol. Chem.* **276**, 5265-5273.
- Lippincott-Schwartz, J. and Phair, R. D. (2010). Lipids and cholesterol as regulators of traffic in the endomembrane system. *Annu. Rev. Biophys.* **39**, 559-578.
- Lippincott-Schwartz, J., Altan-Bonnet, N. and Patterson, G. H. (2003). Photobleaching and photoactivation: following protein dynamics in living cells. *Nat. Cell Biol.* **2003 Suppl.**, S7-S14.
- Maxfield, F. R. and McGraw, T. E. (2004). Endocytic recycling. *Nat. Rev. Mol. Cell Biol.* **5**, 121-132.
- McCaffrey, M. W., Bielli, A., Cantalupo, G., Mora, S., Roberti, V., Santillo, M., Drummond, F. and Bucci, C. (2001). Rab4 affects both recycling and degradative endosomal trafficking. *FEBS Lett.* **495**, 21-30.
- Miaczynska, M., Christoforidis, S., Giner, A., Shevchenko, A., Uttenweiler-Joseph, S., Habermann, B., Wilm, M., Parton, R. G. and Zerial, M. (2004). APPL proteins link Rab5 to nuclear signal transduction via an endosomal compartment. *Cell* **116**, 445-456.
- Murphy, R. F. (1991). Maturation models for endosome and lysosome biogenesis. *Trends Cell Biol.* **1**, 77-82.
- Ober, R. J., Martínez, C., Lai, X., Zhou, J. and Ward, E. S. (2004a). Exocytosis of IgG as mediated by the receptor, FcRn: an analysis at the single-molecule level. *Proc. Natl. Acad. Sci. USA* **101**, 11076-11081.
- Ober, R. J., Martínez, C., Vaccaro, C., Zhou, J. and Ward, E. S. (2004b). Visualizing the site and dynamics of IgG salvage by the MHC class I-related receptor, FcRn. *J. Immunol.* **172**, 2021-2029.
- Pagano, A., Crottet, P., Prescianotto-Baschong, C. and Spiess, M. (2004). In vitro formation of recycling vesicles from endosomes requires adaptor protein-1/clathrin and is regulated by rab4 and the connector rabaptin-5. *Mol. Biol. Cell* **15**, 4990-5000.
- Patterson, G. H. and Lippincott-Schwartz, J. (2002). A photoactivatable GFP for selective photolabeling of proteins and cells. *Science* **297**, 1873-1877.
- Pfeffer, S. and Aivazian, D. (2004). Targeting Rab GTPases to distinct membrane compartments. *Nat. Rev. Mol. Cell Biol.* **5**, 886-896.
- Popov, S., Hubbard, J. G., Kim, J., Ober, B., Ghetie, V. and Ward, E. S. (1996). The stoichiometry and affinity of the interaction of murine Fc fragments with the MHC class I-related receptor, FcRn. *Mol. Immunol.* **33**, 521-530.
- Prabhat, P., Ram, S., Ward, E. S. and Ober, R. J. (2004). Simultaneous imaging of different focal planes in fluorescence microscopy for the study of cellular dynamics in three dimensions. *IEEE Trans. Nanobioscience* **3**, 237-242.
- Prabhat, P., Gan, Z., Chao, J., Ram, S., Vaccaro, C., Gibbons, S., Ober, R. J. and Ward, E. S. (2007). Elucidation of intracellular recycling pathways leading to exocytosis of the Fc receptor, FcRn, by using multifocal plane microscopy. *Proc. Natl. Acad. Sci. USA* **104**, 5889-5894.
- Raghavan, M., Bonagura, V. R., Morrison, S. L. and Björkman, P. J. (1995). Analysis of the pH dependence of the neonatal Fc receptor/immunoglobulin G interaction using antibody and receptor variants. *Biochemistry* **34**, 14649-14657.
- Ram, S., Prabhat, P., Chao, J., Ward, E. S. and Ober, R. J. (2008). High accuracy 3D quantum dot tracking with multifocal plane microscopy for the study of fast intracellular dynamics in live cells. *Biophys. J.* **95**, 6025-6043.
- Ram, S., Prabhat, P., Ward, E. S. and Ober, R. J. (2009). Improved single particle localization accuracy with dual objective multifocal plane microscopy. *Opt. Express* **17**, 6881-6898.
- Rink, J., Ghigo, E., Kalaidzidis, Y. and Zerial, M. (2005). Rab conversion as a mechanism of progression from early to late endosomes. *Cell* **122**, 735-749.
- Roopenian, D. C. and Akilesh, S. (2007). FcRn: the neonatal Fc receptor comes of age. *Nat. Rev. Immunol.* **7**, 715-725.
- Schonteich, E., Wilson, G. M., Burden, J., Hopkins, C. R., Anderson, K., Goldenring, J. R. and Prekeris, R. (2008). The Rip11/Rab11-FIP5 and kinesin II complex regulates endocytic protein recycling. *J. Cell Sci.* **121**, 3824-3833.
- Schuster, M., Lipowsky, R., Assmann, M. A., Lenz, P. and Steinberg, G. (2011). Transient binding of dynein controls bidirectional long-range motility of early endosomes. *Proc. Natl. Acad. Sci. USA* **108**, 3618-3623.
- Sheff, D. R., Daro, E. A., Hull, M. and Mellman, I. (1999). The receptor recycling pathway contains two distinct populations of early endosomes with different sorting functions. *J. Cell Biol.* **145**, 123-139.
- Sönnichsen, B., De Renzis, S., Nielsen, E., Rietdorf, J. and Zerial, M. (2000). Distinct membrane domains on endosomes in the recycling pathway visualized by multicolor imaging of Rab4, Rab5, and Rab11. *J. Cell Biol.* **149**, 901-914.
- Stenmark, H. (2009). Rab GTPases as coordinators of vesicle traffic. *Nat. Rev. Mol. Cell Biol.* **10**, 513-525.
- Taraska, J. W., Perrais, D., Ohara-Imaizumi, M., Nagamatsu, S. and Almers, W. (2003). Secretory granules are recaptured largely intact after stimulated exocytosis in cultured endocrine cells. *Proc. Natl. Acad. Sci. USA* **100**, 2070-2075.
- Traer, C. J., Rutherford, A. C., Palmer, K. J., Wassner, T., Oakley, J., Attar, N., Carlton, J. G., Kremerskothen, J., Stephens, D. J. and Cullen, P. J. (2007). SNX4 coordinates endosomal sorting of TfR with dynein-mediated transport into the endocytic recycling compartment. *Nat. Cell Biol.* **9**, 1370-1380.
- Tsuboi, T. and Rutter, G. A. (2003). Multiple forms of "kiss-and-run" exocytosis revealed by evanescent wave microscopy. *Curr. Biol.* **13**, 563-567.
- Ullrich, O., Reinsch, S., Urbé, S., Zerial, M. and Parton, R. G. (1996). Rab11 regulates recycling through the pericentriolar recycling endosome. *J. Cell Biol.* **135**, 913-924.
- Vaccaro, C., Zhou, J., Ober, R. J. and Ward, E. S. (2005). Engineering the Fc region of immunoglobulin G to modulate in vivo antibody levels. *Nat. Biotechnol.* **23**, 1283-1288.
- van der Sluijs, P., Hull, M., Webster, P., Mâle, P., Goud, B. and Mellman, I. (1992). The small GTP-binding protein rab4 controls an early sorting event on the endocytic pathway. *Cell* **70**, 729-740.
- Ward, E. S. and Ober, R. J. (2009). Chapter 4: Multitasking by exploitation of intracellular transport functions: the many faces of FcRn. *Adv. Immunol.* **103**, 77-115.
- Ward, E. S., Martínez, C., Vaccaro, C., Zhou, J., Tang, Q. and Ober, R. J. (2005). From sorting endosomes to exocytosis: association of Rab4 and Rab11 GTPases with the Fc receptor, FcRn, during recycling. *Mol. Biol. Cell* **16**, 2028-2038.
- Yao, X., Zhang, J., Zhou, H., Wang, E. and Xiang, X. (2012). In vivo roles of the basic domain of dynein p150 in microtubule plus-end tracking and dynein function. *Traffic* **13**, 375-387.
- Yoshida, M., Claypool, S. M., Wagner, J. S., Mizoguchi, E., Mizoguchi, A., Roopenian, D. C., Lencer, W. I. and Blumberg, R. S. (2004). Human neonatal Fc receptor mediates transport of IgG into luminal secretions for delivery of antigens to mucosal dendritic cells. *Immunity* **20**, 769-783.
- Zerial, M. and McBride, H. (2001). Rab proteins as membrane organizers. *Nat. Rev. Mol. Cell Biol.* **2**, 107-117.
- Zhou, J., Mateos, F., Ober, R. J. and Ward, E. S. (2005). Conferring the binding properties of the mouse MHC class I-related receptor, FcRn, onto the human ortholog by sequential rounds of site-directed mutagenesis. *J. Mol. Biol.* **345**, 1071-1081.
- Zoncu, R., Perera, R. M., Balkin, D. M., Pirruccello, M., Toomre, D. and De Camilli, P. (2009). A phosphoinositide switch controls the maturation and signaling properties of APPL endosomes. *Cell* **136**, 1110-1121.